J. Biomed. Eng. Res : 427-433, 2010

New Seed Detection by Shape Analysis for Construction of Vascular Structures

Hackjoon Shim[1], Hyunjoon Lee[1], Il Dong Yun[2], and Sang Uk Lee[1]

[1]*School of Electrical Engineering, Automation and Systems Research Institute (ASRI)*
BK21 Research Division for Information Technology
[2]*Department of Digital and Information Engineering, Hankuk University of Foreign Studies*
(Received October 11, 2010. Accepted December 1, 2010)

Abstract

Although tracking methods are efficient and popular for vessel segmentation, they require a seed to initiate an instance of tracking. In this paper, a new method to detect new seeds for tracking of arterial segments from CT angiography (CTA) and to construct a vascular structure is proposed. The proposed algorithm is based on shape analysis of connected components in a volume of interest around a vessel segment which was already extracted by tracking. The eigenvalues of the covariance matrix are used as the shape features for detection. The experimental results on actual clinical data showed that the results totally revealed the arterial tree not hindered by bone or veins. In visual comparison to a method which combines registration and subtraction of both pre-contrast and post-contrast CT volumes, the proposed method produced comparable results to the reference method and were confirmed of its feasibility for clinical use of reducing the cost and burden of patients.

Key words : CT angiography, tracking, seed detection, shape analysis

Ⅰ. INTRODUCTION

Quantification of morphology of vascular structures from CT angiography (CTA) images is very important, because cardiovascular diseases and cerebro-vascular diseases are the first and fifth causes of death among all kinds of causes [1] and many of them are related with abnormalities in vessels, such as aneurism, stenosis, calcification, and so on. Explosive increase in the number of CT images has enabled radiologists to examine these abnormalities [2], but at the same time it brought about the need for automation of segmentation of vascular structures. Among many segmentation algorithms of vascular structures [3], tracking-based techniques [4-7] focus on directly extracting the vessel centerline and cross-sectional boundaries and they are, thus, relatively robust to cluttered background and low signal-to-noise ratios.

Furthermore, examination of the radius of vessel lumen along the extracted centerline allows for detection of vascular abnormalities which show abrupt change in the lumen radius. However, tracking-based methods require an initial condition, which is often termed a seed, for each vessel segment, construction of vascular structures is very challenging. There have been numerous approaches to address this issue [6, 8-10].

Chen and Molloi [8] constructed three dimensional (3-D) vascular structures through thinning and skeleton pruning. They used CT angiograms of porcine hearts as the input. This work employed a global threshold for binarization prior to the thinning process and, therefore, cannot circumvent shortcomings of the global threshold. Cerebral ateries of human beings are more complicated than coronary arteries of pigs and they often exist in the vicinity of bones and veins. Because arteries have intensity distributions overlapped with those of bones and veins in CT angiograms, simple binarization using global thresholds often fails in segmentation of arterial vascular structures.

Shim *et al*. [6] have partitioned a CTA volume into the upper and lower sub-volumes and extracted cerebral arteries with a separate algorithm applied to each sub-volume, i. e. adaptive tracking method to the lower sub-volume and thresholding-based region growing to the upper sub-volume. As a consequence, it has inconsistency in methods over the whole volume, which results in discontinuities between the lowest slice of the upper sub-volume and the highest one of

Corresponding Author : Hackjoon Shim
School of Electrical Engineering, Automation and Systems Research Institute (ASRI) BK21 Research Division for Information Technology
Seoul National University, Seoul, 151-742, Korea
Tel : +82-2-880-8394 / Fax : +82-2-880-8220
E-mail : hjshim@diehard.snu.ac.kr

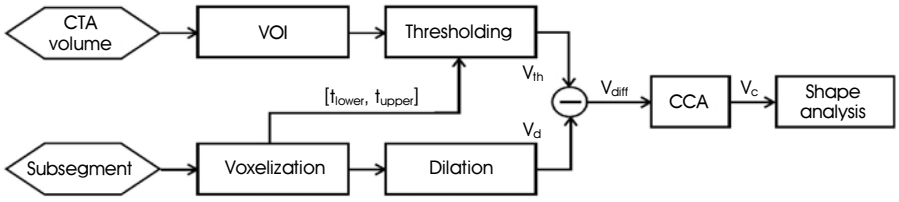

Fig. 1. The block diagram for detection of new seeds

the lower sub-volume. This work also suffers from the same drawbacks of global thresholds in the upper sub-volume.

In Al-Kafai *et al.*'s work [9], seed points were detected by seeking local maxima intensity values over a coarse grid. They used adaptive thresholding to filter out false detections that are due to noise or imaging artifacts. The input images of this work are confocal microscope images which are 2-D, and, accordingly, this work is not suitable to 3-D images of CT angiography.

On the while, Hong *et. al* [10] revealed cerebro-vascular structures by eliminating bones in brain. They used two CT image volumes of a patient which had been scanned before and after injection of contrast agent, respectively. The two CT volumes were rigidly registered to each other and then the pre-contrast volume was subtracted from the post-contrast one. This approach works much better than the others and, thus, is used as a reference in visual comparative evaluation of the performance of our algorithm. However, it requires twice of scanning which doubles the radiation exposure and cost for patients and suffers from motion artifacts.

In this paper, a new method is proposed to detect seeds for tracking of arterial segments which takes into account not only intensity values of individual pixels but also shape features of pixel groups. The experimental results with actual CT angiograms of brain and heart showed construction of vascular structures witch are comparable to the registration-subtraction results [10] using both the pre-contrast and post-contrast CT volumes.

II. Methods

Since the proposed method aims to detect new seeds, it assumes that some vessel segments have been extracted by one of tracking algorithms [4-7]. Neighborhood of each vessel segment is examined in sequential steps along its centerline to detect new seeds. The block diagram in Figure 1 illustrates how new seeds are detected for each sub-segment. The following subsections will describe each block of Figure 1 grouping some related blocks together.

A. Generation of volume of interest (VOI) and thresholding

Figure (2a) shows a single vessel segment which was already tracked and is composed of N elliptical cross-sections. The vessel segment is divided into N_{sub} sub-segments and each sub-segment is examined to see if there is any new seed around it. Adjacent sub-segments are supposed to overlap with each other so that seeds near the frontal and back ends of the sub-segment should not be missed. Empirically, N_{sub}= 61 and the number of overlapped cross-sections, N_{over}= 30 which means that almost every cross-section is checked twice for new seed detection.

Three sub-segments are exemplified in Figure (2a) and the

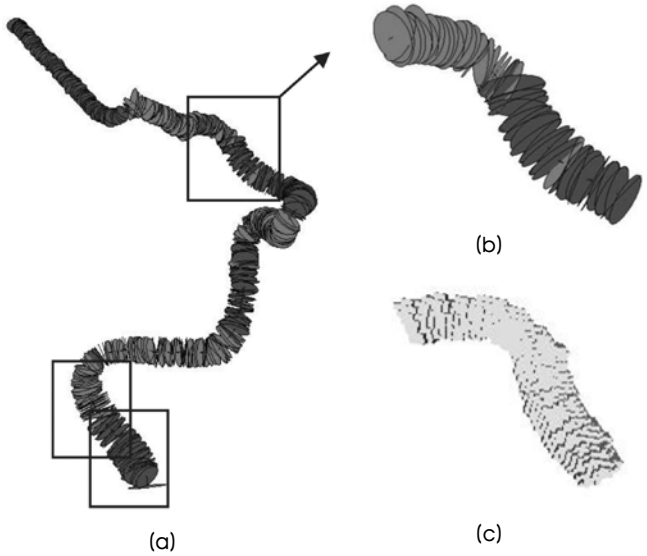

Fig. 2. Division of a vessel segment into sub-segments which are overlapped with adjacent ones: (a) generation of a sub-segment in each volume of interest (VOI) which is represented by a black box, (b) enlargement of the cross-sections of a specific sub-segment which is enclosed by the black box denoted by the arrow, (c) the solid sub-segment voxelized from the cross-sections of (b) by filling every gap between the adjacent cross-sections.

volume of interest (VOI) including each of them is denoted by a black box. The one with the arrow is enlarged in Figure (2b) and (2c). Figure (2b) shows the cross-sections which constitute the sub-segment in more detail. A solid sub-segment is generated by voxelization of the cross-sections of Figure (2b) into triangular meshes [11].

Then, the VOI including the sub-segment is thresholded to exclude other voxels than vessels. Since global threhsolds often fail in separation of arteries from bones and vein contamination, we computed the thresholds using local statistics of the arterial sub-segment, i.e., the mean μ and the standard deviation σ of the intensity distribution. As previously stated, the sub-segment is obtained by voxelization of N_{sub} elliptical cross-sections and is assumed to have HU values of Gaussian distribution. Two asymmetric thresholds are defined by

$$t_{lower} = \mu - \alpha\sigma,\ t_{upper} = \mu + \beta\sigma, \qquad (1)$$

where α and β determine the range of intensities to which the new sub-segment should belong. t_{lower} is the threshold between bones and arteries, because bones usually have higher HU values. On the contrary, t_{lower} separates arteries from other tissues of lower HU values. Since the bone distribution can be more easily separated from the artery, t_{upper} is set to be farther from the mean μ than t_{lower}, which means that $\beta > \alpha$. Empirically we established $\alpha = 1$ and $\beta = 2$ so that the interval $[t_{lower}, t_{upper}]$ may include about 80% of voxels in the sub-segment by the assumption of Gaussian distribution. Figure (3a) is the thresholding result represented by V_{th} in Figure 1.

B. Dilation of a sub-segment and subtraction

If the voxelized volume of Figure (2c) is subtracted from V_{th}, that is, the thresholding of the VOI, only the voxels which have intensity values in the interval $[t_{lower}, t_{upper}]$ and at the same time do not belong to the sub-segment. To ensure that the sub-segment is removed completely in the subtraction result V_{diff}, before subtraction, the voxelized volume is dilated with a spherical structuring element of radius r_{dil}, which is empirically set to 3. Figure (3b) shows the dilated voxelization result V_d and Figure (3c) displays the binary subtraction result represented by $V_{diff} = V_{th} - V_d$. Now, we should find elongated connected components which are expected to be parts of a vessel segment that is not tracked yet.

C. Shape analysis of the remaining components

The voxels in the binary volume V_{diff} have the intensity values in $[t_{lower}, t_{upper}]$, but simultaneously do not belong to the current arterial sub-segment. On that account, new seeds should be detected among the connected components in the volume V_c which is obtained by connected component analysis (CCA) of V_{diff}. Each connected component $C = \{(x_i, y_i, z_i | i = 1, ..., N_c)\}$ in V_c is analyzed to see whether it includes a new seed or not. In other words, it should be long enough to be considered as part of a new vessel segment. Accordingly, only the connected component having the longest path-length longer than a threshold t_L should be analyzed. According to its shape, we established three categories of tube-like objects, blob-like objects, and plate-like objects and classified a component C into one of them. Then the tube-like one is selected as a new vessel segment. More specifically, its classification depends on the eigenvalues $\{\lambda_1, \lambda_2, \lambda_3\}$ of the covariance matrix P of C.

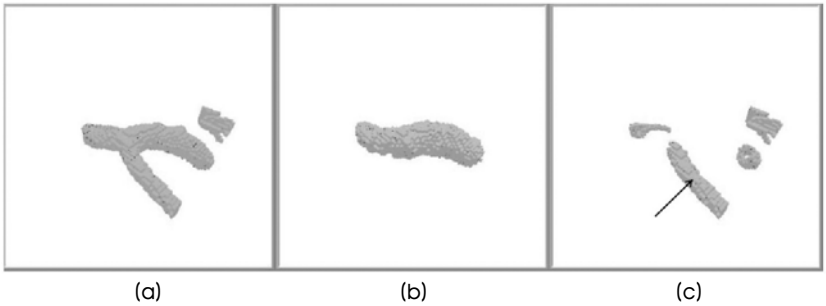

Fig. 3. Processing to detect new seeds in VOI(Volume of Interest) : (a) thresholding result using local statistics, V_{th}, (b) dilated voxelization of the arterial sub-segment, V_d, (c) difference between (a) and (b), $V_{diff} = V_{th} - V_d$.

$$PX_j = \lambda_j X_j, \text{ where } j = 1, 2, 3 \text{ and } P = \begin{pmatrix} \sigma_{xx} \sigma_{xy} \sigma_{xz} \\ \sigma_{yx} \sigma_{yy} \sigma_{yz} \\ \sigma_{zx} \sigma_{zy} \sigma_{zz} \end{pmatrix}. \quad (2)$$

The eigenvalues are ordered according to their magnitudes as $|\lambda_1| \geq |\lambda_2| \geq |\lambda_3|$. The relationship between the object shape and the relative magnitude of eigenvalues is illustrated in Figure 4.

To measure the vesselness of the component C, two ratios R_a and R_b are defined as

$$R_a = \frac{|\lambda_2|}{|\lambda_1|}, \; R_b = \frac{\sqrt{|\lambda_2 \lambda_3|}}{|\lambda_1|} = \sqrt{\frac{|\lambda_2|}{|\lambda_1|}} \sqrt{\frac{|\lambda_3|}{|\lambda_1|}}. \quad (3)$$

R_a and R_b are very similar to the geometric ratios defined in [12], but are more intuitive, since they can be factorized into the product of the relative ratios of the eigenvalue magnitudes as eq. (3). Both of them are between [0,1]. R_b differentiates the blob-like object from both the plate-like and tube-like objects. If it approaches to 1, it means $|\lambda_1| \simeq |\lambda_2| \simeq |\lambda_3|$, and the component C is blob-like. On the other hand, R_a is used to distinguish between the plate-like and the tube-like objets. If it is close to 1, the component is considered as a plate-like object. Conversely if $R_a \simeq 0$, it is a tube-like object and finally is selected to have a new seed inside. Compactly the selection of the component C can be represented as

$$\text{Longest-pathlength}(C) > t_L, \; R_a < t_{R_a}, \text{ and } R_b < t_{R_a}. \quad (4)$$

The new initial seed is defined as the centroid of contact surface between the component and the artery sub-segment. The initial direction for the new tracking is set to the eigenvector x_1 corresponding to λ_1.

Ⅲ. Experiments

The proposed segmentation method has been tested with actual clinical data provided by Seoul National University Bundang Hospital. The dataset is composed of four pairs of pre-contrast and post-contrast brain CT images. The reconstruction thickness/interval is $1.0/0.5\,\mathrm{mm}$ and the contrast agent injection is $4-5\ \mathrm{ml/sec}$ and $100-120\ \mathrm{ml}$ for the post-contrast CT volumes.

At first, four initial conditions were placed to initiate four instances of tracking for the left and right internal carotid arteries (ICA) and the left and right vertebral arteries (VA). The tracking algorithm previously devised by Shim et al. [7] extracted four vessel segments and then the seed detection algorithm proposed in this paper automatically discovered new seeds for further extraction of vessel segments. Combination of tracking and seed detection was recursively iterated three times and finally constructed cerebra-vascular structures.

Since each dataset has the pre-contrast and the post-contrast series, the proposed method was compared visually to the registration-subtraction method [10] using both the pre-contrast and post-contrast volumes, which has been performed using 3-D registration and bone subtraction.

Additionally, the proposed algorithm was performed on one cardiac CT angiogram to extract coronary arteries, i. e. right coronary artery (RCA), left anterior descending artery (LDA), and left circumflex artery (LCX). Since a heart beats all the time, registration is not so simple as in brain images, so the registraion-subtraction method [10] cannot be used as a reference. Instead, a commercial software modularized in

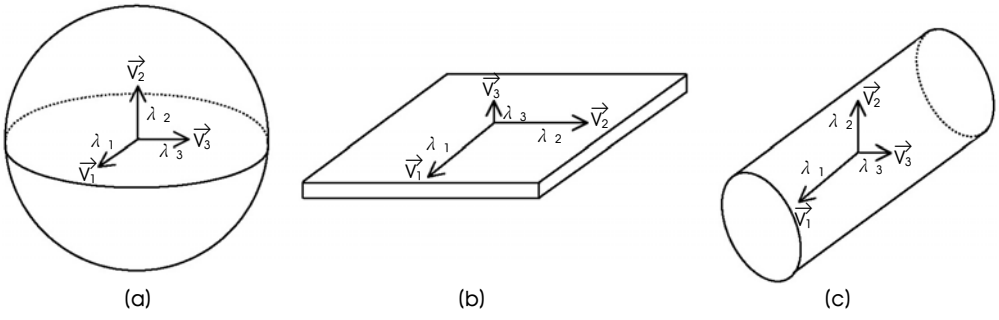

Fig. 4. The relationship between an object shape and the magnitudes of the eigenvalues of the covariance matrix: (a) blob-like object ($|\lambda_1| \simeq |\lambda_2| \simeq |\lambda_3|$), (b) plate-like object ($|\lambda_1| \simeq |\lambda_2| \gg |\lambda_3|$), (c) tube-like object($|\lambda_1| \gg |\lambda_2| \simeq |\lambda_3|$).

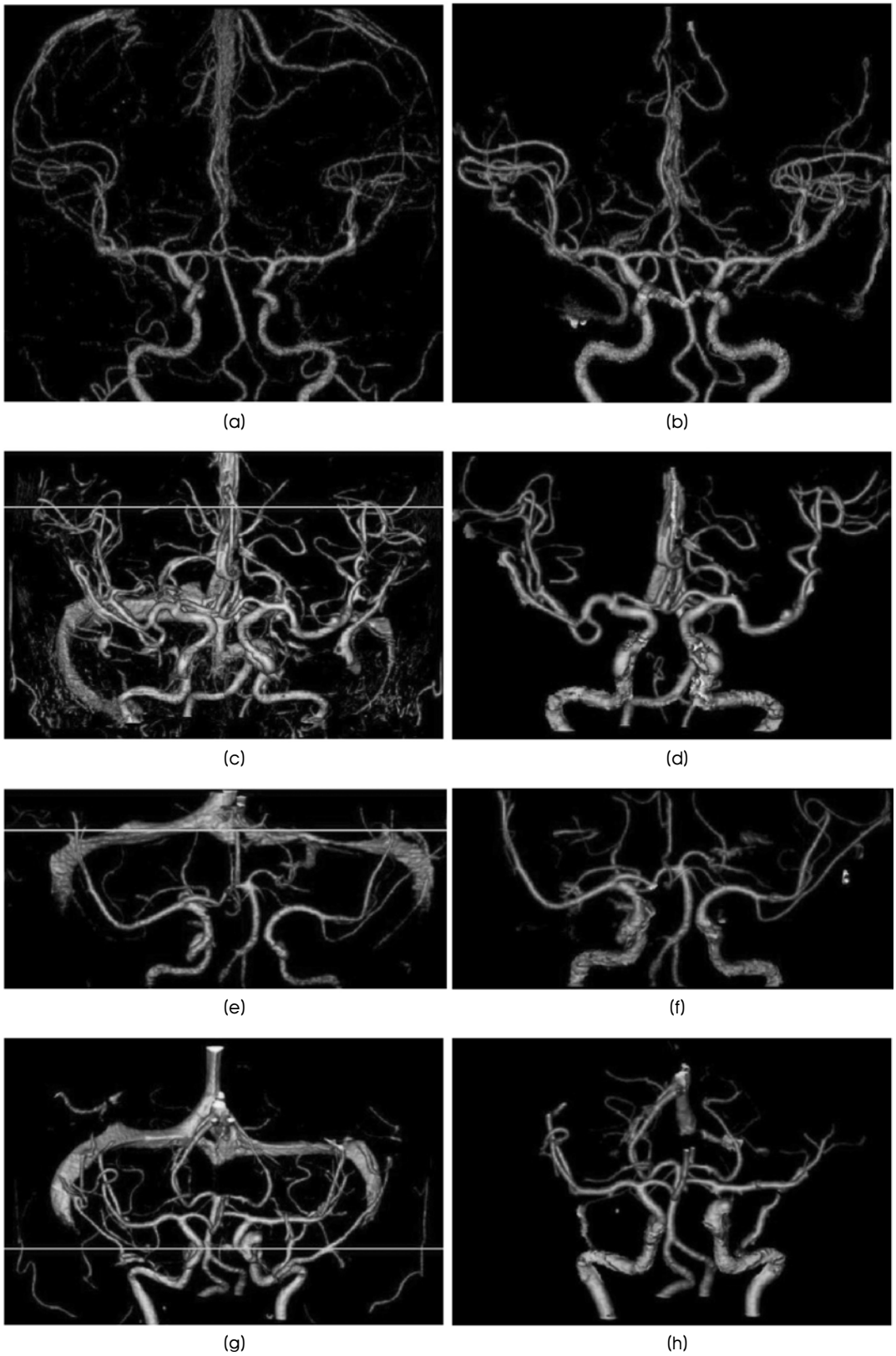

Fig. 5. Visual comparison for performance evaluation on brain CT images: (a), (c), (e), (g) the results of the tegistration-subtracion method [10], (b), (d), (f), (h) the results of the proposed method.

Philips Brilliance™ workstation was employed as a reference for visual comparison.

Ⅳ. Discussion

The overall segmentation results for the four datasets were mostly satisfying in that most of main arteries of the Circle of Willis have been extracted. Figure 5 illustrated the visual comparison of the segmentation results of the proposed method to the Registration-Subtraction results for the four datasets. Figures (5a), (5c), (5e), and (5g) correspond to the registration-subtraction results and show quite clearly the cerebro-vascular structures including arteries. However, they require double-scanning and have the inevitable drawbacks of the large motion artefact and vein contamination.

The results of the proposed method are shown in Figures (5b), (5d), (5f), and (5h). Though they reveal some broken vessel segments and missing ones, each of them exhibits the vessel tree structure evidently. The missing segments might be tracked by additional user interaction or using the prior anatomical knowledge. Additionally the thick veins in the registration-subtraction results which are not related to aneurysms have been removed and this led to improvement in the visibility of only the arterial tree structure. As a result, the segmentation results of the proposed method in Figures (5b), (5d), (5f), and (5h) can be asserted to be comparable to the corresponding registration-subtraction results in Figures (5a), (5c), (5e), and (5g).

A radiologist who is expert on cerebral vascular structure evaluated the results and commented that they were comparable to the registration-subtraction results and could be even better for examination of tiny vessels in the sense that the proposed segmentation is not so much affected by the motion artefact as the registration-subtraction method [10].

Additionally, application of the proposed method to a cardiac CT also built cardio-vascular structures (Figure (6b)) compatible with the commercial software of Philips (Figure (6a)).

In conclusion, we proposed a new seed detection algorithm based on shape analysis of the connected components in a VOI around a vessel segment which had been already extracted by tracking. The eigenvalues of the covariance matrix were used as the shape features for the detection. The experimental results on actual clinical data showed that the results of the proposed method totally revealed the arterial tree not hindered by bone or veins. Furthermore, the thick veins of no interest were removed in the results. Since the registration-subtraction method requires scanning twice, the proposed method has the advantages of reducing the cost and burden of patients, while it maintains the quality of segmentation results as comparable to the reference method [1]. In addition, the segmentation result itself is significant for computer assisted diagnosis (CAD), because it is used as coarse input to a more accurate modelling scheme such as [13].

REFERENCES

[1] World Health Organization, “Annex Table 2: Deaths by cause,

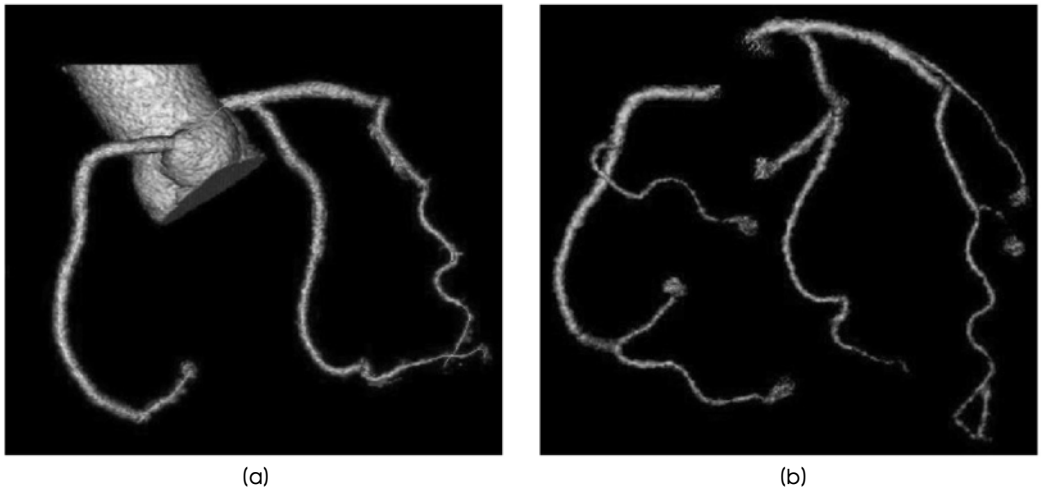

(a) (b)

Fig. 6. Visual comparison for performance evaluation on a cardiac CT image: (a) the result of a commercial software of Philips, (b) the result of the proposed method.

sex and mortality stratum in WHO regions, estimate for 2002," The *World Health Report*, 2004.

[2] K. H. Lee, H. J. Lee, J. H. Kim, H. S. Kang, K. W. Lee, H. Hong, H. J. Chin, and K. S. Ha, "Managing the CT data explosion: initial experiences of archiving volumetric datasets in a mini PACS," *Journal of Digital Imaging*, vol. 18, pp. 188-195, 2005.

[3] D. Lesage, E. D. Angelini, I. Bloch, and G. Funka-Lea, "A review of 3D vessel lumen segmentation techniques: models, features, and extraction schemes," *Medical Image Analysis*, vol. 13, pp. 819-845, 2009.

[4] O. Wink, W. J. Niessen, and M. A. Viergever, "Fast Delineation and Visualization of Vessels in 3-D Angiographic Images," *IEEE Trans. on Medical Imaging*, vol. 19, pp. 337-346, 2000.

[5] C. Florin, N. Paragious, and J. Williams, "Globally optimal active contours, sequential Monte-Carlo and on-line learning for vessel segmentation," *Proceedings of European Conference on Computer Vision (ECCV)*, pp. 476-489, 2006.

[6] H. Shim, I. D. Yun, K. M. Lee, and S. U. Lee, "Partition-based extraction of cerebral arteries from CT angiography with emphasis on adaptive tracking," *Lecture Notes in Computer Science, Information Processing in Medical Imaging(IPMI)*, vol. 3565, pp. 357-368, Jul. 2005.

[7] H. Shim, D. Kown, I. D. Yun, and S. U. Lee, "Robust segmentation of cerebral arterial segments by a sequential Monte-Carlo method: particle filtering," *Computer Methods and Programs in Biomedicine*, vol. 84, pp. 135-145, 2006.

[8] Z. Chen and S. Molloi, "Automatic 3D vascular tree construction in CT angiography," *Computerized Mdeical Imaging and Graphics*, vol. 27, pp. 469-479, 2003.

[9] K. A. Al-Kofahi, A. Can, S. Lasek, D. H. Szarwski, N. Dowell-Mesfin, W. Shain, J. N. Turner, and B. Roysam, "Medican-based robust algorithms for tracing neurons from noisy confocal microscope images," *IEEE Trans. on Information Technology in Biomedicine*, vol. 7, pp. 302-317, 2003.

[10] H. Hong, H. Lee, Y. G. Shin, and Y. H. Seong, "Three-Dimensional Brain CT-DSA using Rigid Registration and Bone Masking for Early Diagnosis and Treatment Planning," *Lecture Note on Artificial Intelligence*, vol. 3398, 3rd Asian Simulation Conference, Jeju Island, Korea, October. 2004, pp. 167-176.

[11] T. P. Fang and L. A. Piegl, "Delanay Triangulation in Three Demensions," *IEEE Trans. on Computer Graphics and Applications*, vol. 15, pp. 62-69, 1995.

[12] A. F. Frangi, W. J. Niessen, K. L. Vincken, and M. A. Viergever, "Multiscale vessel enhancement filtering," *Lecture Notes in Computer Science*, vol. 1496, Medical Image Computing and Computer-Assisted Intervention(MICCAI), Boston, USA, pp. 130-137, Oct. 1998.

[13] I. Volkau, W. Zheng, R. Baimouratov, A. Aziz, and W. L. Nowinski, "Geometric modeling of the human normal cerebral arterial system, *IEEE Trans. on Medical Imaging*," vol. 24, pp. 529-539, 2005.